

1 **Captions**

2 Supporting information

3

4 **Supporting information 1a.** Samples' selection and preparation.

5

6 **Supporting information 1b.** Human and animal bone CNS isotope data, preservation
7 indicators and anthropological information available.

8

9 **Supporting information 2.** AMS data and models

10

11 **Supporting information 3.** Radiogenic Sr data

12

13 **Supporting information 4.** Dental calculus microremains

14

15 **Supporting information 5.** Details of aDNA analyses conducted on Les Bréguières individuals
16 and mitochondrial SNPs consensus profiles obtained for positive samples

17

18 **Supporting information 6.** Summary of multidisciplinary data

19

20

21 **Supporting information (SI)**

22

23 Supporting information 1a. Samples' preparation.

24 Collagen extraction was performed on chunk bones by using a modified protocol from Richards
25 and Hedges (1999). Samples are demineralised in 0.5 M HCl at 5°C, then soaked in NaOH
26 overnight at room temperature and solubilised with HCl pH 3 at 70°C during 48h. Solubilized
27 collagen is filtered with EzeeFilter® device, frozen at -65°C in glass vials and then freeze-dried
28 during 2 days. Elemental composition and stable isotope ratios (C, N, S) are measured by EA-
29 IRMS (Europa Scientific elemental analyser coupled to Europa Scientific 20-20 IRMS; Iso-
30 Analytical, Crewe, UK). Laboratory standards used are calibrated against IAEA international
31 standard for all measurements; measurement error is 0.1‰ for carbon and nitrogen and 0.2‰
32 for sulphur.

33 In total, enamel from 32 teeth of 21 human individuals and 7 teeth from fauna (*Lepus europaeus*
34 and *Erinaceus* sp.) were sampled for strontium isotope analysis (SI 3). Two dental pieces from
35 11 human individuals were sampled, while from the remaining 10 individuals only one tooth
36 was. Second and third molars were preferentially selected in those cases in which two teeth per
37 individual were sampled and second molars in case only one tooth per individual was accessible
38 for sampling. When second molars were not available, premolars or canines were chosen ideally
39 instead, while first molars were always discarded to avoid any possible interference of enamel
40 mineralized during the breastfeeding and/or weaning periods (Hillson, 1996).

41 Sample preparation and analysis were carried out directly in the Clean Labs and Isotope
42 Facilities of the University of Cape Town, South Africa. Prior to analysis, a chunk of enamel
43 of ca. 20mg from each tooth was cut in a longitudinal way to reflect all mineralization stages
44 of the dental piece. These pieces of enamel were cleaned by abrasion and dentine was removed
45 completely, rinsed and ultrasonicated for 20 minutes in MilliQ water. The diamond drill bits
46 used for this process were cleaned with ethanol and ultrasonicated in MilliQ water between
47 samples to avoid cross-contamination (Budd et al., 2000). A subsample of each enamel piece
48 was taken for Sr concentration in order to check for diagenesis. Following this, in a Clean Lab,
49 the remaining chunks of cleaned enamel samples were digested with 2mL bi-distilled 65%
50 HNO₃ in a closed Teflon beaker placed on a hotplate at 140 °C for an hour. After this, digested
51 samples were dried and redissolved in 1.5 mL of bi-distilled 2M HNO₃ before being
52 centrifuged at 4000 rpm for 20 minutes. The resulting supernatant was then collected for

53 strontium separation chemistry. At this last step, a subsample from each sample was used to
54 calculate the concentration with ^{88}Sr intensity (V) regression equation built with SRM987
55 standard from NIST (National Institute of Standards and Technology, Gaithersburg, MD,
56 USA). The isolation of strontium as carried out with 200 μl of Eichrom Sr.Spec resin loaded in
57 Bio-Spin Disposable Chromatography Bio-Rad Columns following the method described in
58 Pin et al. (1994). The strontium fraction separated this way for each sample was then dried
59 down dissolved in 2 ml 0.2% bi-distilled HNO_3 and diluted to 200 ppb Sr concentrations for
60 the isotope analysis. A NuPlasma HR multicollector inductively-coupled-plasma mass
61 spectrometer (MC-ICP-MS) was used to measure the $^{87}\text{Sr}/^{86}\text{Sr}$ ratios. Sample analyses were
62 referenced to bracketing analyses of SRM987, using a $^{87}\text{Sr}/^{86}\text{Sr}$ reference value of 0.710255
63 from NIST. All strontium isotope data were corrected for isobaric rubidium interference at 87
64 amu using the measured signal for ^{85}Rb and the natural $^{85}\text{Rb}/^{87}\text{Rb}$ ratio. The instrumental mass
65 fractionation was corrected using the measured $^{87}\text{Sr}/^{86}\text{Sr}$ ratio and the exponential law, as well
66 as a true $^{86}\text{Sr}/^{88}\text{Sr}$ value of 0.1194. Results of repeated analyses of an in-house carbonate
67 standard processed and measured with the batches of samples in this study ($^{87}\text{Sr}/^{86}\text{Sr} =$
68 0.708943; 2 sigma 0.000042; n=33) are in agreement with long-term results for this in-house
69 standard ($^{87}\text{Sr}/^{86}\text{Sr}$; 0.708915; 2 sigma 0.000047; n=125). Furthermore, one blank was added
70 for every two batches in order to double check the cleanliness of the sample preparation.

71

Supporting information 1b. Human and animal bone CNS isotope data, preservation indicators and anthropological information available.

Tables are presented according to the sampling groups: sexed coxal bones (DSP; Murail et al. 2005), adult skull/mandible and immature skull/mandible (according to previous anthropological study; Provost 2013; Provost et al. 2017). * indicates individuals with calculus microremains tested (* did not provide result; ** only 1 microremain identified; *** several/diversity of microremains identified; see sup. mat. 4).

Sample Code (Animal)	Species	Yield (mg/g)	%C	%N	d ¹³ C _{V-PDB}	d ¹⁵ N _{Air}	C/N	%S	d ³⁴ S _{V-CDT}	C/S	N/S
Br 383	Sheep	113.5	39.4	13.7	-20.4	6.9	3.4	0.2	12.0	524.0	156.2
Br 173	Sheep	62.3	40.3	14.4	-21.2	5.7	3.3	0.2	12.5	536.0	164.2
Br 117	Sheep	51.1	39.5	14.0	-20.2	4.3	3.3	0.2	10.2	525.4	159.6
Br_F1 os	Sheep	44.7	43.0	15.3	-20.4	4.1	3.3				
Br 194	Goat	74.2	38.0	13.4	-20.4	4.3	3.3	0.2	12.1	505.4	152.8
Br 545	<i>Bos</i> sp.	129.7	40.1	14.2	-22.0	5.4	3.3				
Br_F2A	<i>Bos</i> sp.	85.7	37.2	13.2	-21.5	6.1	3.3				
Br_F2B	<i>Bos</i> sp.	46.6	40.7	14.4	-21.4	5.6	3.3				
Br_F3 os	Wild boar	35.0	37.8	13.2	-20.3	5.1	3.3				
Br 243	<i>Sus</i> sp	47.4	39.8	14.1	-20.3	4.8	3.3	0.2	10.9	529.3	160.7
Br 245	<i>Sus</i> sp	60.7	39.5	13.9	-20.3	4.7	3.3	0.2	11.4	525.4	158.5
Br_F5	Dog	25.4	42.5	15.2	-19.3	10.0	3.2				
Br 378	Red deer	115.1	44.9	16.1	-21.2	5.4	3.2	0.2	12.1	597.2	183.5
Br_F4	Horse	79.4	42.8	15.3	-21.6	5.0	3.2				

Sample Code (Human coxal bone)	Sex	Age (yrs)	Yield (mg/g)	%C	%N	d ¹³ C _{V-PDB}	d ¹⁵ N _{Air}	C/N	%S	d ³⁴ S _{V-CDT}	C/S	N/S
Br 3695	M	>30	104.1	40.2	14.4	-20.0	9.4	3.2	0.2	10.4	534.7	164.2
Br 3680	M		57.8	39.8	14.4	-20.1	9.6	3.3	0.2	10.9	529.3	164.2

Br 3515	M		67.9	39.1	14.0	-18.1	11.1	3.2	0.2	11.4	520.0	159.6
Br 3737	M	20-59	72.3	40.8	14.3	-19.9	9.3	3.3	0.2	11.9	542.6	163.0
Br 3688	M	>30	61.4	34.7	12.1	-20.1	9.4	3.3	0.2	11.5	461.5	137.9
Br 3660	M	>40	12.3	37.4	13.2	-19.5	9.6	3.3				
Br 3670	M		80.7	32.3	11.3	-19.8	8.9	3.3	0.2	11.9	429.6	128.8
Br 19	M	30-49	81.7	41.9	14.8	-20.1	9.2	3.3	0.2	10.6	557.3	168.7
Br 3740	F	>40	71.4	41.7	14.8	-19.8	8.9	3.3	0.2	11.6	554.6	168.7
Br 3712	F	>50	99.3	36.0	13.1	-19.9	9.1	3.2	0.1	10.0	957.6	298.7
Br 3668	F		66.8	36.3	12.7	-19.8	9.3	3.3	0.2	11.0	482.8	144.8
Br 3733	F	>50	76.6	41.7	14.9	-19.7	9.5	3.2	0.2	11.7	554.6	169.9
Br 3710	F		68.8	40.0	14.2	-19.9	10.1	3.3	0.2	11.2	532.0	161.9
Br 3739	F		92.2	32.9	11.5	-19.8	8.9	3.3	0.2	9.8	437.6	131.1
Br 3708	F	>30	87.9	36.0	12.7	-19.9	9.5	3.3	0.2	11.9	478.8	144.8
Br 3723	F		70.9	40.1	14.5	-19.8	9.1	3.2	0.2	14.6	533.3	165.3
Br 3696	F	>50	72.4	35.3	12.7	-19.9	9.4	3.2	0.2	14.6	469.5	144.8

Sample Code (Human adult skull/mandible)	Yield (mg/g)	%C	%N	d ¹³ C _{V-PDB}	d ¹⁵ N _{Air}	C/N	%S	d ³⁴ S _{V-CDT}	C/S	N/S
Br H22 4239**	54.5	35.6	12.8	-20.1	9.4	3.2	0.2	14.7	473.5	145.9
Br H28 3220***	74.9	40.2	14.7	-18.9	10.7	3.2	0.2	13.5	534.7	167.6
Br H29 3240***	69.0	38.4	13.8	-19.8	10.3	3.2	0.2	13.4	510.7	157.3
Br H16 3252***	70.2	30.2	10.8	-20.0	9.3	3.2	0.1	13.3	803.3	246.2
Br H09 3256***	63.9	32.3	11.4	-19.6	9.9	3.3	0.1	14.5	859.2	259.9
Br H20 3236**	94.9	40.5	14.5	-19.5	10.2	3.2	0.2	14.2	538.7	165.3
Br H06 3368***	51.9	36.8	13.1	-19.9	9.5	3.3	0.2	14.3	489.4	149.3
Br H20 bis	73.8	41.7	14.5	-19.8	9.3	3.2	0.2	13.2	554.6	165.3
Br H5 3269**	78.3	37.8	13.5	-19.9	10.5	3.3	0.2	14.0	502.7	153.9
Br H32 3260*	58.7	40.8	14.5	-19.9	9.1	3.3	0.2	10.4	542.6	165.3

Br H10 3237	64.4	41.1	14.5	-19.9	10.2	3.3	0.2	14.1	546.6	165.3
Br HNN2 3249	107.9	42.3	15.0	-19.6	10.3	3.3	0.2	14.5	562.6	171.0
Br HNN4 3311	50.7	40.9	14.7	-19.8	10.9	3.2	0.2	14.0	544.0	167.6
Br H27 0027	51.4	29.2	10.1	-19.9	9.9	3.3	0.1	15.0	776.7	230.3
Br H33 0033	39.4	30.9	10.6	-20.0	9.1	3.4	0.1	14.3	821.9	241.7
Br H23 0023		36.9	13.3	-19.9	9.3	3.4	0.2	9.3	490.8	151.6
Br H26 3239	65.7	41.7	14.9	-19.8	9.8	3.2	0.2	10.6	554.6	169.9
Br H19 0019**	66.8	40.0	13.9	-20.3	9.2	3.3	0.2	10.9	532.0	158.5
Br H3 3709 bis (2011)	75.3	40.6	14.5	-20.0	9.0	3.2				

Sample Code (Human immature skull/mandible)	Yield (mg/g)	%C	%N	$\delta^{13}\text{C}_{\text{V-PDB}}$	$\delta^{15}\text{N}_{\text{Air}}$	C/N	%S	$\delta^{34}\text{S}_{\text{V-CDT}}$	C/S	N/S
Br H04 3386	67.2	39.5	14.1	-19.8	9.8	3.2	0.2	10.8	525.4	160.7
Br H02 3317	105.8	41.6	14.9	-19.8	9.8	3.3	0.2	12.3	553.3	169.9
Br H08 0008	40.8	41.0	15.0	-20.0	9.8	3.2	0.2	12.5	545.3	171.0
Br H31 3218**	87.3	41.0	14.8	-20.0	10.3	3.2	0.2	9.9	545.3	168.7
Br H12 3231	47.2	33.1	11.8	-20.0	9.9	3.3	0.1	10.5	880.5	269.0
Br H07 3354	40.1	40.8	14.5	-19.9	9.3	3.3	0.2	10.2	542.6	165.3
Br H14 0014	38.1	38.8	13.7	-20.1	9.2	3.3	0.2	9.6	516.0	156.2
Br H01 3337*	103.7	41.8	15.2	-19.8	9.2	3.2	0.2	11.5	555.9	173.3
Br H12A 3437	96.7	40.9	14.7	-19.7	8.9	3.2	0.2	11.6	544.0	167.6
Br H12B 0012B	125.0	42.5	15.2	-20.1	9.3	3.2	0.2	11.8	565.3	173.3
Br 3256 bis	75.7	42.1	15.1	-19.3	9.9	3.2	0.2	6.4	559.9	172.1
Br HNN7 3742	96.4	42.1	15.1	-19.2	9.7	3.2	0.2	12.9	559.9	172.1
Br HNN8 4077	68.6	33.8	12.0	-20.0	9.9	3.3	0.1	9.1	899.1	273.6
Br H03 3709	52.5	31.7	11.3	-19.7	9.5	3.3	0.2	12.5	421.6	128.8
Br HNN5 3466	64.7	32.9	11.6	-19.7	9.6	3.3	0.2	11.0	437.6	132.2

Br HNN1 2716	61.2	39.7	14.2	-20.1	9.6	3.2	0.2	9.8	528.0	161.9
Br HNN6 3710 3427	9.3	40.9	14.5	-19.9	9.6	3.3	0.2	10.1	544.0	165.3

Supporting information 2. AMS data and models

AMS ¹⁴C dates from Mougins – Les Bréguières samples. The modelled individual dates are represented by the highest posterior density region (HPD). * One new date have been obtained thanks to the ongoing project INTERACT (ANR-17-FRAL-0010).

Sample reference	Field reference (Sechter, unpublished)	Stratigraphic attribution (Sechter, unpublished)	Phase (this study)	AMS Laboratory reference	Conventional age BP	Standard error	Dated material	Species	anatomical identification	Calibrated date BCE (95%)	Modelled date BCE (HPD 95%)	Reference
BRG#CH_1	BR_C1	C1	C1	LTL-15033A	5966	45	Carbonized vegetal matter	Unspecified	unspecified	[-4954 ; -4725]	[-4500; -4101]	Provost et al., 2017
BRG_3356	BR_H09	C2	C2-C4	LTL-13783A	5581	45	Bone collagen	<i>Homo sapiens</i>	skull fragment	[-4492 ; -4344]	[-4635; -4293]	Provost et al., 2017
BRG_3386	BR_H04	C2	C2-C4	LTL-17555A	5799	45	Bone collagen	<i>Homo sapiens</i>	skull fragment	[-4775 ; -4541]	[-4829; -4525]	This study
BRG_3269	BR_H05	C2	C2-C4	LTL-17553A	6367	45	Bone collagen	<i>Homo sapiens</i>	skull fragment	[-5469 ; -5229]	[-4859; -4338]	This study
BRG_3709	BR_H03	C2	C2-C4	LTL-17556A	6395	45	Bone collagen	<i>Homo sapiens</i>	skull fragment	[-5471 ; -5310]	[-4859; -4332]	This study
BRG_3368	BR_H06	C2	C2-C4	LTL-12317A	5870	45	Bone collagen	<i>Homo sapiens</i>	skull fragment	[-4840 ; -4613]	[-4835; -4537]	Provost et al., 2017
BRG_0008	BR_H08	C2	C2-C4	LTL-18523A	5920	35	Bone collagen	<i>Homo sapiens</i>	skull fragment	[-4894 ; -4714]	[-4852; -4590]	This study*
BRG_3386	BR_H04	C2	C2-C4	LTL-8484A	6144	45	Bone collagen	<i>Homo sapiens</i>	skull fragment	[-5215 ; -4963]	[-4829; -4525]	Provost et al., 2017
BRG_3317	BR_H02	C3	C2-C4	LTL-17554A	5860	45	Bone collagen	<i>Homo sapiens</i>	skull fragment	[-4834 ; -4606]	[-4831; -4518]	This study
BRG_3437	BR_H12A	C4	C2-C4	LTL-17545A	5934	45	Bone collagen	<i>Homo sapiens</i>	skull fragment	[-4931 ; -4716]	[-4903; -4739]	This study
BRG_0012B	BR_H12B	C4	C2-C4	LTL-17546A	6111	45	Bone collagen	<i>Homo sapiens</i>	skull fragment	[-5209 ; -4933]	[-4919; -4744]	This study
BRG_3231	BR_H12	C4	C2-C4	LTL-17549A	6215	45	Bone collagen	<i>Homo sapiens</i>	skull fragment	[-5300 ; -5052]	[-4918; -4740]	This study
BRG_3236	BR_H20(1)	C5	C5	LTL-12315A	5864	45	Bone collagen	<i>Homo sapiens</i>	skull fragment	[-4836 ; -4611]	[-4988 -4795]	Provost et al., 2017
BRG_3236	BR_H20(1)	C5	C5	LTL-17550A	5958	45	Bone collagen	<i>Homo sapiens</i>	skull fragment	[-4943 ; -4723]	[-4988 -4795]	This study
BRG_3220	BR_H28	C5	C5	LTL-12316A	5964	45	Bone collagen	<i>Homo sapiens</i>	skull fragment	[-4950 ; -4724]	[-5033; -4808]	Provost et al., 2017

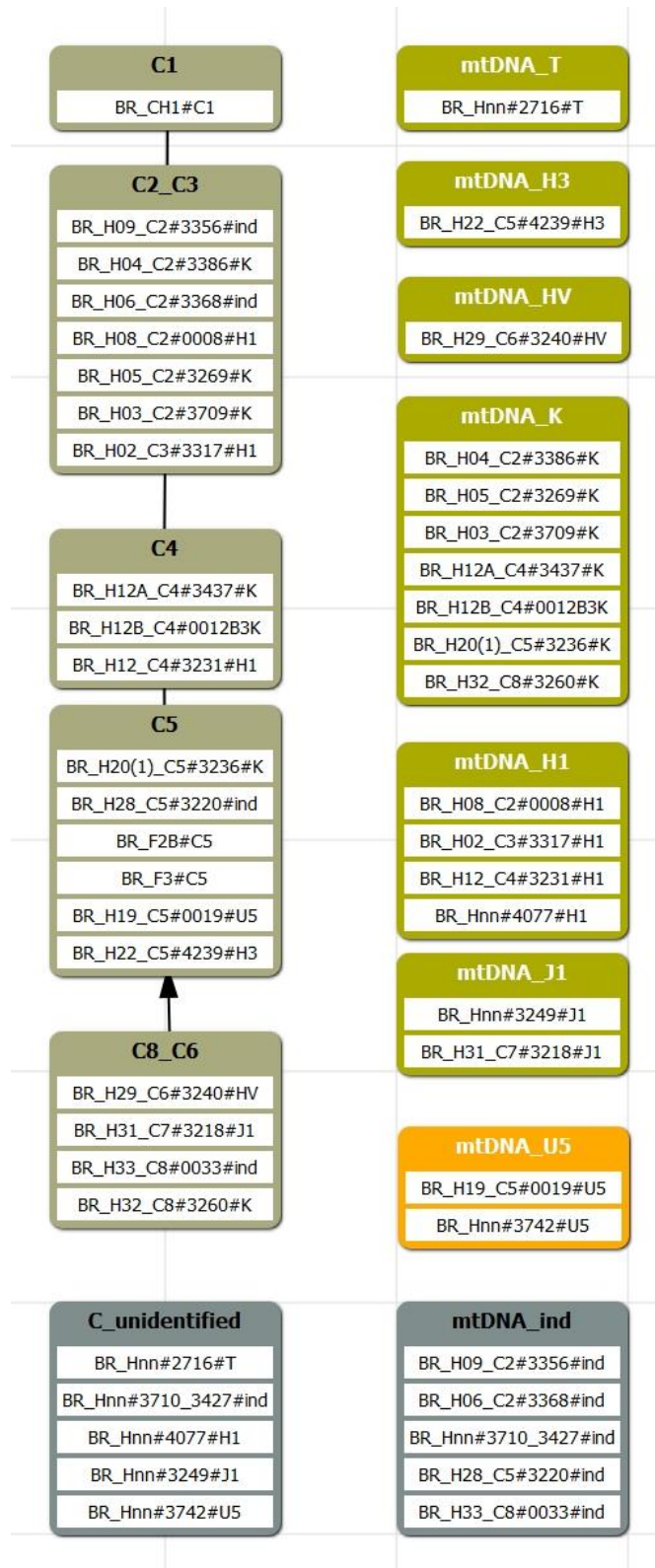
BREG#F2b	BR_C5	C5	C5	LTL-8483A	5971	45	Bone collagen	<i>Bos sp.</i>	skull fragment	[-4962 ; -4728]	[-5035; -4811]	Provost et al., 2017
BREG#F3	BR_C5	C5	C5	LTL-8479A	6032	45	Bone collagen	<i>Ovis aries</i>	skull fragment	[-5044 ; -4825]	[-5057; -4826]	Provost et al., 2017
BRG_0019	BR_H19	C5	C5	LTL-8482A	6104	45	Bone collagen	<i>Homo sapiens</i>	skull fragment	[-5208 ; -4910]	[-5105; -4841]	Provost et al., 2017
BRG_4239	BR_H22	C5	C5	LTL-17560A	6413	45	Bone collagen	<i>Homo sapiens</i>	skull fragment	[-5472 ; -5319]	[-5148; -4828]	This study
BRG_3240	BR_H29	C6	C8-C6	LTL-17551A	6024	45	Bone collagen	<i>Homo sapiens</i>	skull fragment	[-5027 ; -4798]	[-5431; -4920]	This study
BRG_3218	BR_H31	C7	C8-C6	LTL-17548A	6197	45	Bone collagen	<i>Homo sapiens</i>	skull fragment	[-5294 ; -5035]	[-5399; -4990]	This study
BRG_0033	BR_H33	C8	C8-C6	LTL-13780A	6101	45	Bone collagen	<i>Homo sapiens</i>	skull fragment	[-5207 ; -4860]	[-5409; -4947]	Provost et al., 2017
BRG_3260	BR_H32	C8	C8-C6	LTL-13784A	6151	45	Bone collagen	<i>Homo sapiens</i>	skull fragment	[-5218 ; -4964]	[-5379; -4973]	Provost et al., 2017
BRG_2716	BR_HNN1	Unknown	Unkown	LTL-17547A	5793	45	Bone collagen	<i>Homo sapiens</i>	skull fragment	[-4767 ; -4533]	[-4883; -4400]	This study
BREG#3710_3427	BR_HNN6	Unknown	Unkown	LTL-17557A	6211	45	Bone collagen	<i>Homo sapiens</i>	skull fragment	[-5299 ; -5049]	[-5462; -4867]	This study
BREG#4077	BR_HNN8	Unknown	Unkown	LTL-17559A	6217	45	Bone collagen	<i>Homo sapiens</i>	skull fragment	[-5300 ; -5053]	[-5475; -4857]	This study
BRG_3249	BR_HNN2	Unknown	Unkown	LTL-17552A	6219	45	Bone collagen	<i>Homo sapiens</i>	skull fragment	[-5301 ; -5055]	[-5476; -4868]	This study
BREG#3742	BR_HNN7	Unknown	Unkown	LTL-17558A	6245	45	Bone collagen	<i>Homo sapiens</i>	skull fragment	[-5314 ; -5063]	[-5506; -4904]	This study

Phases	B_MAP	B_HPD (95%)	E_MAP	E_HPD (95%)
Phase C3_C2	-4779	[-4857; -4698]	-4425	[-4604; -4242]
Phase C4	-4847	[-4927; -4771]	-4801	[-4883; -4725]
Phase C5	-5005	[-5153; -4910]	-4875	[-4945; -4792]
Phase C8_C6	-5214	[-5594; -5063]	-5041	[-5194; -4942]
Phase_unknown	-5285	[-5576; -5113]	-4645	[-4883; -4380]

Modelled MtDNA clusters and events from Mougins – Les Bréguières. The beginning (B) and end (E) of clusters K, H1, J1 and U5 are represented by their modes a posteriori (BMAP / EMAP) and by their highest posterior density regions with a confidence of 95% (B_HPD / E_HPD). For the isolated events (HV, H3 and T), only the modelled HPD begin and end are given.

mtDNA	B_MAP	B_HPD (95%)	E_MAP	E_HPD (95%)
event_T	–	-4883	–	-4400
event_H3	–	-5148	–	-4828
event_HV	–	-5431	–	-4920
cluster_K	-5161	[-5379; -4973]	-4602	[-4762; -4274]
cluster_H1	-5137	[-5431; -4846]	-4713	[-4808; -4485]
cluster_J1	-5219	[-5481; -45041]	-5110	[-5317; -4913]
cluster_U5	-5243	[-5453; -4947]	-4973	[-5110; -4830]
cluster_unknown	-5197	[-5490; -5008]	-4431	[-4630; -4293]

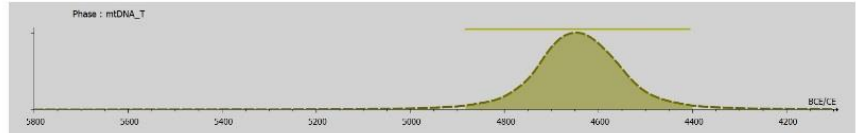
Model of phases built for Mougins – Les Bréguières AMS dates and modelled mtDNA clusters and isolated events. The constraints are only applied on groups of events with available information on relative stratigraphic position.



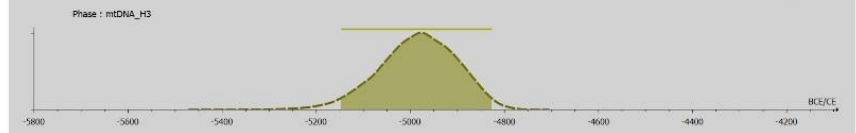
ChronoModel 2.0.18

Modelled mtDNA clusters and isolated events from Mougins – Les Bréguières. The mode a posteriori (MAP) is used as a terminus post quem (TPQ) of modelled phases.

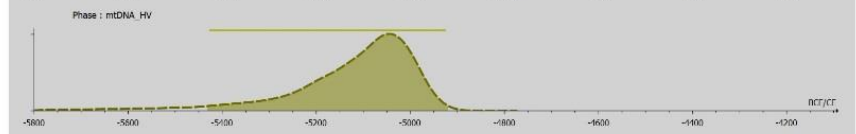
MtDNA_T (n=1)



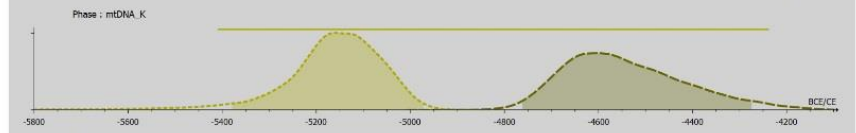
MtDNA_H3 (n=1)



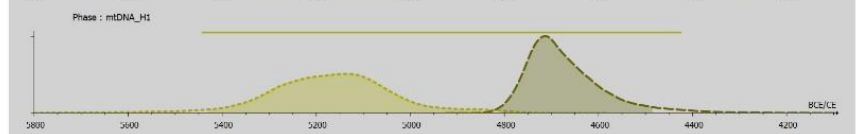
MtDNA_HV (n=1)



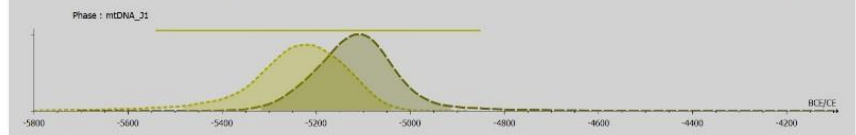
**MtDNA_K (n=7)
TPQ (BMAP): c. 5160 BCE**



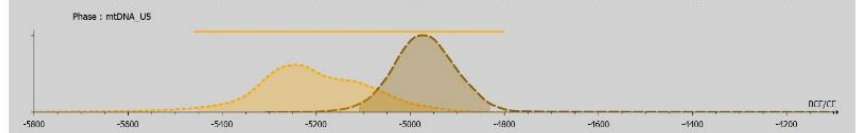
**MtDNA_H1 (n=4)
TPQ (BMAP): c. 5140 BCE**



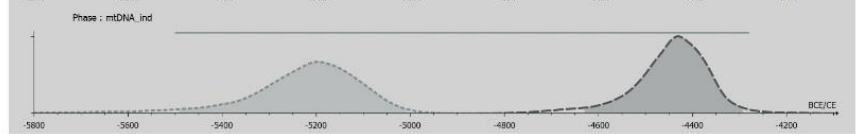
**MtDNA_J1 (n=2)
TPQ (BMAP): c. 5220 BCE**



**MtDNA_U5 (n=2)
TPQ (BMAP): c. 5240 BCE**



**MtDNA_unknown (n=5)
TPQ (BMAP): c. 5200 BCE**



ChronoModel 2.0.18

Supporting information 3. Radiogenic Sr data

Radiogenic Sr data of humans, animals and IRHUM database samples. Human life period correspond to tooth growth period; details provided in associated tables (growth periods estimated according to Alqhatani et al. 2010).

Human tooth sampled for $^{87}\text{Sr}/^{86}\text{Sr}$	Median age- cups outline complete	Median age - crown completed	Life period
I2	1.5	5	Infancy (1)
C	1.5	5.5	Infancy (1)
P3	3.5	5.5	Childhood (2)
P4	3.5	7.5	Childhood (2)
M2	4.5	8	Childhood (2)
M3	8.5	17.5	Adolescence (3)

S-UCT	Lab code	Species/Soil/Plant	Tooth/Location	$^{87}\text{Sr}/^{86}\text{Sr}$	Human life period
20107	Bre-H01 3337	Human	P3	0.7093	2
20133	Bre-H12A 3437	Human	M2 max L	0.7087	2
20108	Bre-H02 3317	Human	I2 max R	0.7096	1
20109	Bre-H05 3269	Human	M2 max R	0.7088	2
20110	Bre-H05 3269	Human	M3 max L	0.7086	3
20111	Bre-H6A	Human	M2 max R	0.7085	2
20112	Bre-H6A	Human	M3 max R	0.7086	3
20113	Bre-H6B	Human	M2 mand L	0.7085	2
20114	Bre-H6B	Human	M3 mand L	0.7085	3
20115	Bre-H07 3354	Human	M2 max R	0.7087	2
20116	Bre-H07 3354	Human	M3 max R	0.7089	3
20117	Bre-H09 3356	Human	M2 mand L	0.7083	2
20118	Bre-H09 3356	Human	M3 mand L	0.7083	3
20119	Bre-H16 3252	Human	M2 mand R	0.7081	2
20120	Bre-H19 0019	Human	M2 mand L	0.7082	2
20121	Bre-H19 0019	Human	M3 mand L	0.7083	3
20122	Bre-H20 0020	Human	P4 max L	0.7094	2
20123	Bre-H20 0020	Human	M3 mand R	0.7088	3
20124	Bre-H20bis	Human	M2 mand R	0.7086	2
20125	Bre-H22 4239	Human	P4 mand L	0.7087	2
20126	Bre-H26 3239	Human	C max L	0.7088	1
20128	Bre-H29 3240	Human	M2 mand L	0.7090	2
20129	Bre-H29 3240	Human	M3 mand L	0.7091	3

20130	Bre-H31 3218	Human	I2 mand L	0.7090	1
20127	Bre-H28 3220	Human	I2 max R	0.7086	1
20131	Bre-H32 3260	Human	M2 mand R	0.7102	2
20132	Bre-H32 3260	Human	M3 mand R	0.7100	3
20134	Bre-H/3428	Human	P4 mand L	0.7086	2
20135	Bre-H/3428	Human	M3 mand L	0.7087	3
20136	Bre-H/6302	Human	M3 max R	0.7095	2
20137	Bre-H/6356	Human	C max R	0.7086	1
20138	Bre-H/6356	Human	P3 max R	0.7086	2
20139	Cod n° 70	European hare	P3 mand L	0.7096	
20140	Cod n° 58	European hare	I1 mand L	0.7095	
20141	Cod n° 57	European hare	P3 mand L	0.7096	
20142	Cod n° 59	European hare	P3 mand L	0.7096	
20143	Cod n° 65	European hare	I1 mand L	0.7091	
20144	Cod n° 38	Hedgehog	M1 mand L	0.7093	
20145	Cod n° 39	Hedgehog	M2 mand L	0.7087	
IRHUM DB France	F13-202	Topsoil	ca. 8km north	0.7079	
IRHUM DB France	F13-202	Grass	ca. 8km north	0.7082	
IRHUM DB France	F13-201	Topsoil	ca. 8km north	0.7082	
IRHUM DB France	F13-201	Grass	ca. 8km north	0.7083	

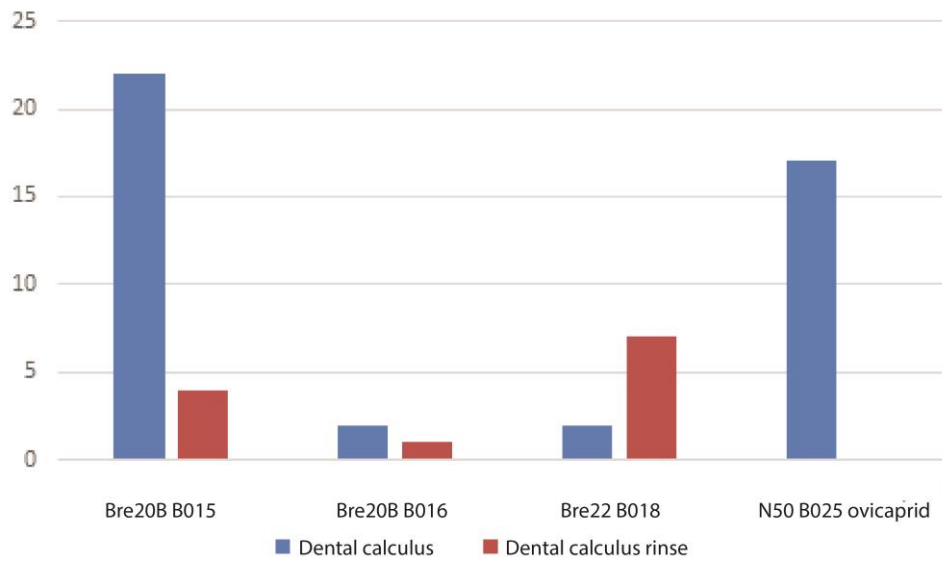
Supporting information 4. Dental calculus microremains

Dental calculus microremains methodology and comparison of interior and exterior dental calculus rinse samples as well as all microremains types found.

Whilst some teeth had medium deposits of supragingival dental calculus, very large deposits were absent. Wherever possible, chunks of supragingival dental calculus, in preference over dental calculus powder, were sampled with a dental curette and then stored in Eppendorf. The samples were then processed in a controlled airflow cabinet at the Department of Human Evolution laboratories in the Max Planck Institute for Evolutionary Anthropology. Researchers have highlighted the potential of decalcifying the outer layer of dental calculus lumps, to remove contaminating soil particles on the exterior (Hardy et al., 2009). Once we had weighed the samples, we trialed this approach on four of the larger dental calculus chunk samples from humans and fauna, by adding 20 µl of 10 % hydrochloric acid (HCl) to each sample for 45 mins. We then ceased the reaction using 1 mL of distilled water and then centrifuged at 2000×g (Rotilabo®-mini-centrifuge with a microcentrifuge rotor) for 10 minutes and pipetted the supernatant. We then agitated the pellet and pipetted the released suspension of microremains and dissolved calculus for mounting, while leaving undigested calculus lump in the tube. We then finished decalcification by adding 25 µl of 10% hydrochloric acid to the calculus samples for 0.5 to 3 hours. The samples were then centrifuged again at 2000×g for 10 minutes, and then about xx100 µl of supernatant was decanted and replaced with distilled water. This was repeated one more time to remove the HCl. After the second decanting, they were refilled with a 25% glycerine solution. We examined each slide under brightfield and cross-polarized light on a Zeiss Axioscope A1 microscope at 400× magnification. All detected microremains were noted and identified when possible, but we focused on identifying those microremains relating to plants. Phytoliths were classified into standard morphotypes, while starches were classified into types defined in this study (Table below). A type may indicate a specific plant family or genus but not in all cases.

To combat laboratory contamination, processing was done in a lab, subject to a weekly regime of laboratory cleaning (see more specifically Power et al., 2014a, 2015, 2016). In addition, we prepared regular blank slides over the course of the analysis (SI 4). Each blank slide was prepared identically to the dental calculus slides.

Number of microremains



Type	Classification	Interpretation
Starches	type 1	endosperm starch-producing plant
	type 2	Triticeae
	type 3	indeterminate plant
	type 5	likely underground storage organ bearing plant
	type 6	
	type 7	indeterminate plant
	type 8	indeterminate plant
	indeterm. starch	indeterminate plant
	dmg	indeterminate plant
	Phytoliths	bilobate
rondel		indeterminate grass
short-cell indeterm.		indeterminate grass
l-c elongate pp		indeterminate grass
trichome		indeterminate grass
hair mono		indeterminate grass
globular rugulate/ echinate		indeterminate dicot
bulliform blocky		indeterminate grass
ovate		
hair indeterm.		indeterminate plant
parallelepiped blocky		indeterminate dicot
parallelepiped thin blocky		
paddle-shape		
oblong trapezoid		
rugulose sub ovoid		indeterminate dicot
plate		indeterminate dicot

	jigsaw	indeterminate dicot
	indeterm.	indeterminate plant
Unsilicified plants	unsilicified conifer	conifer tissue
	monocot unsilicified	indeterminate monocot plant
	dicot unsilicified	indeterminate dicot plant
	tracheid	indeterminate plant
	unsilicified plant hair	indeterminate plant
	indeterm. unsilicified	indeterminate plant
	stellate hair	indeterminate dicot plant
	indeterm. unsilicified stoma	indeterminate plant
	indeterm. diatom	algae
	pennate diatom	benthic diatom (indicating shallow water)
	calcium oxalate	indeterminate plant
Fungal	negraspore	indeterminate fungi
	non-oral fungal spore	indeterminate fungi
	indeterm. spore	indeterminate fungi
	brown spore	indeterminate fungi
	candida or other oral spores	indeterminate fungi
	indeterminate	indeterminate fungi
	barbule	bird feather
	mammal hair	mammal
	mycelium	indeterminate plant
	mycelium with arrow-shapes?	indeterminate plant
	possible cystolith	indeterminate plant
	charcoal	
	cellulose type fibre	lab contaminate
	synthetic fibre	lab contaminate
	textile fibre	lab contaminate
	other	

Supporting information 5. Details of aDNA analyses conducted on Les Bréguières individuals and mitochondrial SNPs consensus profiles obtained for positive samples

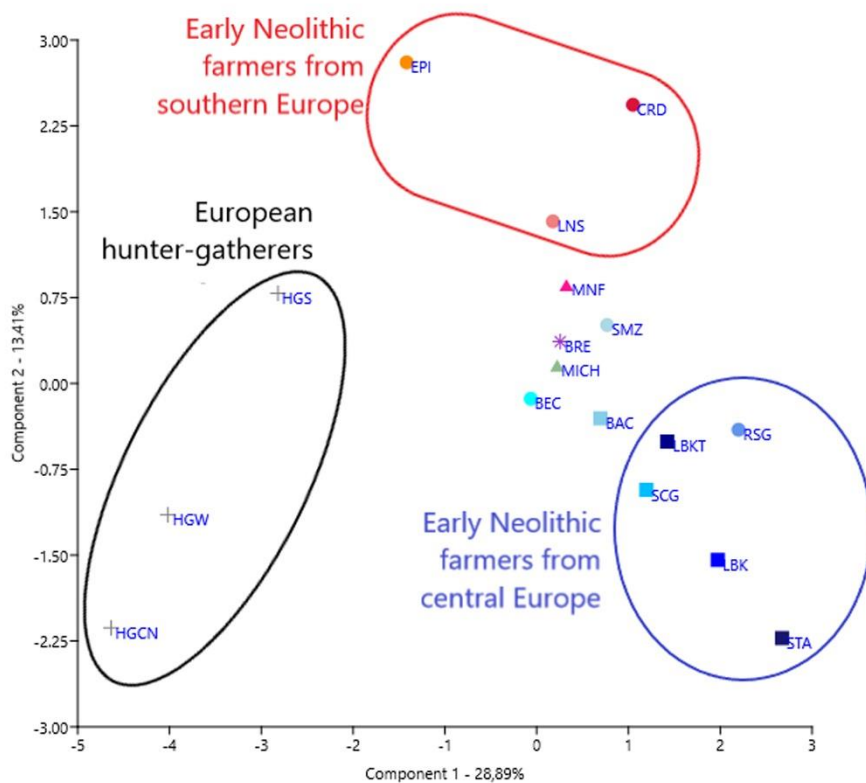
Powder from the inner part of the petrous bones from 30 individuals was collected and submitted to a bleach wash as described in Boessenkool et al. (2017). We then followed the procedure of Mendisco et al. (2011) to extract the DNA using the 'NucleoSpin Extract II kit' (Macherey-Nagel, Düren, Germany). To determine the mitochondrial (mtDNA; maternal) and Y chromosome (paternal) haplogroups for every sample, 18 mitochondrial and 10 Y chromosome SNPs (Single Nucleotide Polymorphisms) were typed through MALDI-TOF MS-based method (iPLEX1Gold technology, Sequenom, Inc., San Diego, CA), as described in Mendisco et al. (2011). Four overlapping fragments of the mtDNA HVS-I control region were also amplified to determine the maternal haplotypes of the individuals (nps 16,024±16,380; see Rivollat et al. 2015 for detailed procedures).

Mitochondrial SNPs consensus profiles obtained for positive samples (black allele A/C/G/T for ancestral allele; red allele A/C/G/T for derived allele; grey for no result)

	M*	N*	N1a	I	W	X	R*	HV*	H	H1(J1)	H3	V	J	T	U*	U4	U5	K	
	10400	10873	13780	10034	3505	6371	12705	14766	2706	3010	6776	4580	12612	1888	11467	11332	13617	10550	
Individual	C/T	C/T	A/G	T/C	A/G	C/T	T/C	T/C	G/A	G/A	T/C	G/A	A/G	G/A	A/G	C/T	T/C	A/G	mtDNA Haplogroup
Breguières_H02_3317	C	T	A		A	C	C	C	A	A	T		A	G	A	C	T	A	H1
Breguières_H3_3709 bis (2011)	C	T	A		A	C	C	T	G	G	T		A	G	G	C	T	G	K
Breguières_H8_0008	C	T	A		A	C	C	C	A	A	T		A	G	A	C	T	A	H1
Breguières_H12A_3437	C	T	A		A	C	C	T	G	G	T	G	A	G	G	C	T	G	K
Breguières_H12B_0012B	C				A		C	C	G	G	T		A		AG	C	T	G	K
Breguières_H19_0019	C		A		A	C	C	T	G	G	T			G	G	C	C	A	U5

Breguières_H26_3239	C		A		A	C	C		G	G	T			G	G	C	T	G	K
Breguières_H29_3240	C	T	A		A	C	C	C	G	G	T	G	A	G	A	C	T	A	HV
Breguières_H32_3260	C	T	A		A	C	C	T	G	G	T	G	A	G	G	C	T	G	K
Breguières_2716_HNN1	C	T	A		A	C	C	T	G	G	T		A	A	A	C	T	A	T
Breguières_H31_3218	C	T	A		A	C	C	T	G	A	T		G		A	C	T	A	J1
Breguières_H12_3231	C	T	A		A	C	C	C	A	A	T		A	G	A	C	T	A	H1
Breguières_H20(1)_3236	C	T	A		A	C	C	T	G	G	T	G	A	G	G	C	T	G	K
Breguières_H22_3249	C	T	A		A	C	C	T	G	G	T	G	G	G	A	C	T	A	J
Breguières_H5_3269	C		A		A	C	C	T	G	G	T			G	G	C	T	G	K
Breguières_H3_3709	C	T	A		A	C	C	T	G	G	T		A	G	G	C	T	G	K
Breguières_3742_HNN7	C	T			A	C		T	G	G	T		A		G	C	C	A	U5
Breguières_4047_HNN8	C		A		A	C	C	C	A	A	T			G	A	C	T	A	H1
Breguières_H22_4239	C		A		A	C	C	C	A	G	C		A	G	A	C	T	A	H3

Principal component analysis (PCA) of the ancient mtDNA dataset performed with haplogroup frequencies (BRE : Bréguières group; HGCN: Hunter-gatherers from Central Europe; HGW: Hunter-gatherers from West Europe; HGS: Hunter-gatherers from South Europe; STA: Starcevo-Koros; LBKT: Linearbandkeramik in Transdanubia; LBK: Linearbandkeramik; CRD: Cardial; EPI: Epicardial Early Neolithic in Spain; RSG: Grossgartach/Planig-Friedberg/Rossen; MNF: Middle Neolithic in France; SCG: Schöningen; MICH: Michelsberg; BAC: Baalberge; LNS: Late Neolithic in Spain; SMZ: Salzmünde; BEC: Bernburg) See details of group constitution in Beau *et al.* 2017.



	H	HV	I	J	K	Other_N	N1a	T	U5	U8	Other_U	V	W	X	others
HGCN	0,00	0,00	0,00	0,00	5,00	0,00	0,00	0,00	60,00	25,00	10,00	0,00	0,00	0,00	0,00
HGW	7,14	0,00	0,00	0,00	0,00	0,00	0,00	0,00	78,57	7,14	7,14	0,00	0,00	0,00	0,00
HGS	42,86	0,00	0,00	0,00	0,00	0,00	0,00	0,00	57,14	0,00	0,00	0,00	0,00	0,00	0,00
STA	7,84	1,96	0,00	11,76	25,49	0,00	5,88	21,57	0,00	0,00	3,92	5,88	3,92	5,88	5,88
LBKT	28,00	2,00	0,00	12,00	14,00	0,00	8,00	26,00	2,00	0,00	2,00	6,00	0,00	0,00	0,00
LBK	17,24	4,31	0,00	11,21	18,97	0,00	12,07	25,86	2,59	0,00	0,86	2,59	2,59	0,86	0,86
CRD	28,57	0,00	0,00	4,76	23,81	14,29	4,76	4,76	4,76	0,00	0,00	4,76	0,00	9,52	0,00
BRE	26,32	5,26	0,00	10,53	42,11	0,00	0,00	5,26	10,53	0,00	0,00	0,00	0,00	0,00	0,00
EPI	40,91	2,27	2,27	4,55	18,18	0,00	0,00	6,82	4,55	0,00	18,18	0,00	0,00	2,27	0,00
RSG	18,92	13,51	0,00	8,11	21,62	0,00	10,81	5,41	5,41	0,00	2,70	8,11	0,00	5,41	0,00
MNF	35,00	0,00	0,00	10,00	18,33	0,00	6,67	5,00	13,33	0,00	3,33	3,33	0,00	5,00	0,00
SCG	15,15	3,03	0,00	15,15	30,30	0,00	3,03	12,12	6,06	0,00	3,03	0,00	9,09	3,03	0,00
MICH	30,00	0,00	0,00	13,33	20,00	0,00	3,33	10,00	16,67	0,00	0,00	0,00	3,33	3,33	0,00
BAC	23,08	3,85	0,00	3,85	19,23	0,00	3,85	23,08	3,85	3,85	3,85	0,00	3,85	7,69	0,00
LNS	15,22	0,00	2,17	8,70	23,91	2,17	0,00	13,04	17,39	0,00	4,35	4,35	2,17	6,52	0,00
SMZ	31,03	3,45	0,00	20,69	10,34	0,00	6,90	6,90	3,45	0,00	10,34	3,45	0,00	3,45	0,00
BEC	23,53	0,00	0,00	0,00	17,65	0,00	0,00	11,76	29,41	0,00	0,00	5,88	5,88	5,88	0,00

Detail of mitochondrial haplogroups frequencies measured for ancient European human groups included in the PCA.

Supporting information 6. Summary of multidisciplinary data

Summary of multidisciplinary data obtained with reliability on human craniofacial remains (isotope ratios, radiocarbon dates, aDNA, dental calculus). In grey the unique complete individual. * sample code use for molecular analysis. Correspondence with field reference (Sechter's excavation) and new anthropological reference (Provost et al. 2017) is provided in both text and tables.

Sample Code*	Age category	Dental calculus	mtDNA haplogroup	AMS ¹⁴ C (Modelled, cal. BCE, HDP 95%)	Chronological phase/cluster	Info from bone CN isotopic ratio	Info from bone S isotopic ratio
Br H09 3256	Adult	several/diversity of microremains identified		[-4635; -4293] BRG_3356 H09	C2-C3	mainly terrestrial protein intake	influence of seashore
Br H04 3386	Immature			[-4829; -4525] BRG_3386 H04	C2-C3	mainly terrestrial protein intake	in the local range
Br H06 3368	Adult	several/diversity of microremains identified		[-4835; -4537] BRG_3368 H06	C2-C3	mainly terrestrial protein intake	influence of seashore
Br H08 008	Immature		H1	[-4852; -4590] BRG_0008 H08	C2-C3	mainly terrestrial protein intake	in the local range
Br H05 3269	Adult	only 1 microremain identified	K	[-4859; -4338] BRG_3269 H05	C2-C3	mainly terrestrial protein intake	influence of seashore
Br H03 3709	Immature		K	[-4859; -4332] BRG_3709 H03	C2-C3	mainly terrestrial protein intake	in the local range
Br H02 3317	Immature		H1	[-4831; -4518] BRG_3317 H02	C2-C3	mainly terrestrial protein intake	in the local range
Br H12A 3437	Immature		K	[-4903; -4739] BRG_3437 H12A	C4	mainly terrestrial protein intake	in the local range
Br H12B 0012B	Immature		K	[-4919; -4744] BRG_0012B H12B	C4	mainly terrestrial protein intake	in the local range
Br H12 3231	Immature		H1	[-4918; -4740] BRG_3231 H12	C4	mainly terrestrial protein intake	in the local range
Br H20 3236	Adult	only 1 microremain identified	K	[-4988 -4795] BRG_3236 H20(1)	C5	mainly terrestrial protein intake	influence of seashore
Br H28 3220	Adult	several/diversity of microremains identified		[-5033; -4808] BRG_3220 H28	C5	possible contribution of marine protein	influence of seashore
Br H19 0019	Adult	only 1 microremain identified	U5	[-5105; -4841] BRG_0019 H19	C5	mainly terrestrial protein intake	in the local range/similar data with coxal bone
Br H22 4239	Adult	only 1 microremain identified	H3	[-5148; -4828] BRG_4239 H22	C5	mainly terrestrial protein intake	influence of seashore
Br H29 3240	Adult	several/diversity of microremains identified	HV	[-5431; -4920] BRG_3240 H29	C6-C8	mainly terrestrial protein intake	influence of seashore
Br H31 3218	Immature	only 1 microremain identified	J1	[-5399; -4990] BRG_3218 H31	C6-C8	mainly terrestrial protein intake	in the local range
Br H33 0033	Adult			[-5409; -4947] BRG_0033 H33	C6-C8	mainly terrestrial protein intake	influence of seashore

Br H32 3260	Adult	did not provide result	K	[-5379; -4973] BRG_3260 H32	C6-C8	mainly terrestrial protein intake	in the local range/could match with coxal bone data – Possible outlier for Sr isotopic data
Br HNN1 2716	Immature		T	[-4883; -4400] BRG_2716 HNN1	C unidentified	mainly terrestrial protein intake	in the local range
Br HNN6 3710 3427	Immature			[-5462; -4867] BREG#3710_3427 HNN6	C unidentified	mainly terrestrial protein intake	in the local range
Br HNN8 4077	Immature		H1	[-5475; -4857] BREG#4077 HNN8	C unidentified	mainly terrestrial protein intake	in the local range
Br HNN2 3249	Adult		J	[-5476; -4868] BRG_3249 HNN2	C unidentified	mainly terrestrial protein intake	influence of seashore
Br HNN7 3742	Immature		U5	[-5506; -4904] BREG#3742 HNN7	C unidentified	mainly terrestrial protein intake	in the local range
Br H03 3709 bis (2011)	Adult		K (Br_03_3709 bis)		C2-C4	mainly terrestrial protein intake	
Br H16 3252	Adult	several/diversity of microremains identified				mainly terrestrial protein intake	influence of seashore
Br H26 3239	Adult		K (Br_26)			mainly terrestrial protein intake	in the local range/could match with coxal bone data
Br H01 3337	Immature	only 1 microremain identified				mainly terrestrial protein intake	in the local range
Br H20 bis	Adult					mainly terrestrial protein intake	influence of seashore
Br H10 3237	Adult					mainly terrestrial protein intake	influence of seashore
Br HNN4 3311	Adult					mainly terrestrial protein intake	influence of seashore
Br H27 0027	Adult					mainly terrestrial protein intake	influence of seashore
Br H23 0023	Adult					mainly terrestrial protein intake	in the local range/could match with coxal bone data
Br H07 3354	Immature					mainly terrestrial protein intake	in the local range
Br H14 0014	Immature					mainly terrestrial protein intake	in the local range
Br 3256 bis	Immature					mainly terrestrial protein intake	probably coming from more inland
Br HNN5 3466	Immature					mainly terrestrial protein intake	in the local range

